

Synthesis and characterization of gold nanoparticles stabilized by palladium(II) phosphine thiol

Floriana Vitale^{a,c}, Rosa Vitaliano^a, Chiara Battocchio^b, Iliara Fratoddi^{a,*},
Emanuela Piscopiello^c, Leander Tapfer^c, Maria Vittoria Russo^a

^a Department of Chemistry, University of Roma "Sapienza" P.le A. Moro, 5-00185 Roma, Italy

^b Department of Physics, INFN, INSTM and CISDiC Unit, University "Roma Tre", Via della Vasca Navale, 84-00146 Rome, Italy

^c ENEA-Brindisi Research Centre, Department of Physics and Technology and New Materials (FIM), S.S. 7 Appia km.713, 72100 Brindisi, Italy

Received 31 October 2007; received in revised form 17 December 2007; accepted 17 December 2007

Available online 28 December 2007

Abstract

This work is focused on the synthesis of innovative hybrids made by linking gold nanoparticles to protected organometallic Pd(II) thiolate. The organometallic protected Pd(II) thiolate, i.e. *trans*-thioacetate-ethynylphenyl-bis(tributylphosphine)palladium(II) has been synthesized, *in situ* deprotected and linked to Au nanoparticles. In this way new hybrid, with a direct link between Pd(II) and Au nanoparticles through a single S bridge, has been isolated. The combination of the organometallic Pd(II) thiol with gold nanoparticles allows the enhancement and tailoring of electronic and optical properties of the new organic–inorganic nano-compound. Single-crystal gold nanoparticles, uniform in shape and size were obtained by applying a modified two-phase method (improved Brust–Schiffrin reaction). In addition, the chemical environment of the Au nanoparticles was investigated and a covalent bonding between Au nanoparticles and the organometallic thiols was observed.

© 2007 Elsevier B.V. All rights reserved.

Keywords: Gold nanoparticles; Organometallic thiolates; Pd(II) complexes

1. Introduction

Gold nanoparticles systems stabilized by organothiols are very interesting for their unique properties and their usefulness in fabrication of different molecular architectures and nanocomposite materials [1] that have applicative potentialities in the different fields of optoelectronics, catalysis, chemical sensors and biosensors [2]. The first synthesis of organothiol monolayer–gold nanoclusters hybrid systems was carried out by Brust to overcome the instability of native colloidal gold solutions [3] opening a new field of self-assembled monolayers. Gold nanoclusters are usually stabilized by organothiols [2]. The covalently bound organothiols monolayers improve solubility and stability and allow them to be functionalized by different electro-

chemically, photophysically and biologically active units [4]. The tailoring of electronic properties of Au nanoparticles can be obtained by tuning the nature of the thiol group and the size [5]. Size-control can be achieved by choosing the suitable Au/S molar ratio [6].

When a capping thiol, covalently bound to the Au nanoparticles, has an additional terminal group, it is possible to assemble a second functionalized molecule to obtain bi- or tri-dimensional networks i.e. scaffolds for the development of nanodevices [7]. Only a few papers deal with aromatic arenethiols as capping agents for gold nanoclusters [8,9] which give rise to structural rigidity and compactness to thiol–gold nanoparticles system [10]. Among metal thio-carboxylates, palladium(II) based complexes have been recently prepared [11] with the aim of exploiting their catalytic properties. In this communication, we propose the innovative functionalization of gold nanoparticles upon the *in situ* deprotection of a Pd(II) thiolate (**1**,

* Corresponding author. Tel.: +39 06 49913182; fax +39 06 490324.

E-mail address: iliana.fratoddi@uniroma1.it (I. Fratoddi).

$[(\text{CH}_3\text{COS})\text{Pd}(\text{PBu}_3)_2(\text{C}\equiv\text{CC}_6\text{H}_5)]$. The proposed new Au–Pd organometallic hybrid **2**, is expected to show interesting optical properties, considering the high luminescence quantum yield recently reported for a Pd(II) containing homologue polymer [12]. In this way it will be possible to extend the functionalization from model molecules to thiols with extended conjugation of the organic moiety that is a characteristic of polymetallaynes [13].

2. Results and discussion

Our approach was to synthesize an organometallic thiolate complex which is able to make a direct bond between Pd(II) and Au nanoparticles through a simple single S-bridge. The purposes of our work were to give more structural rigidity and compactness to gold nanoclusters, due to the aryl moiety. In this way it is possible to explore the advanced perspectives for a novel organometallic thiol–gold nanocluster hybrid system and to envisage the extension to the use of rigid rod thiol derivatized polymetallaynes.

The complex **1**, reported in Scheme 1, was synthesized on purpose, by ligand exchange reaction between the square planar monochloride monoacetylide complex $[\text{ClPd}(\text{PBu}_3)_2(\text{C}\equiv\text{CC}_6\text{H}_5)]$ and KSCOCH_3 .

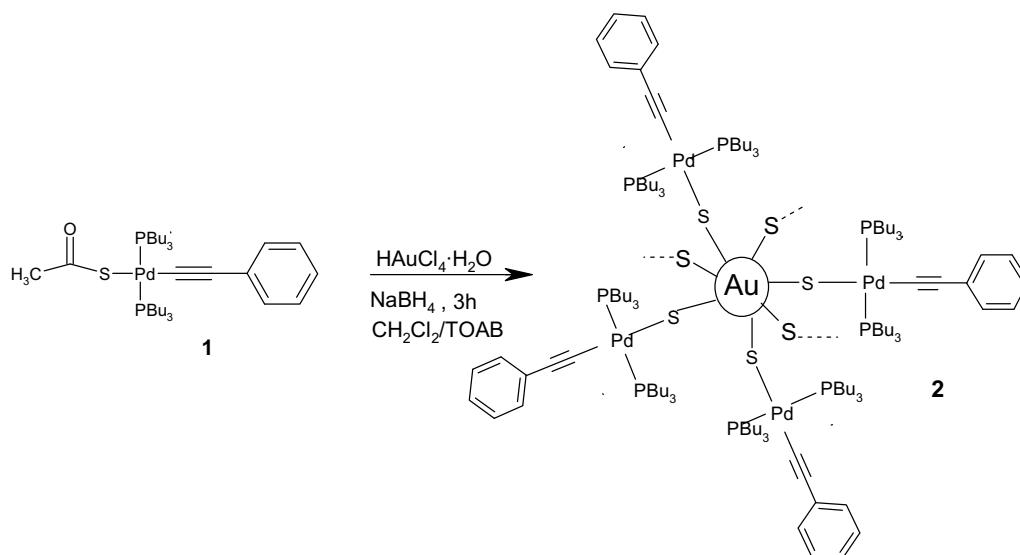
The simple reaction conditions and chemical stability of thiolate organometallic complexes open a new access to the preparation of Pd(II) containing thiolate. Infrared spectra of complex **1** confirmed the proposed structure. The $\text{C}\equiv\text{C}$ stretching mode was found at 2113 cm^{-1} and the protecting acetate showed the carbonyl $\text{C}=\text{O}$ stretching mode at 1627 cm^{-1} . This compound was used for the preparation of a new gold nanocluster hybrid **2** by a single step procedure, in which the deprotection and the anchoring of the thiol group was achieved by covalent bonding.

Gold nanoparticles can be functionalized with complex **1**. In this paper, we report on the synthesis of innovative organometallic stabilized gold nanoparticles. The gold nanoparticles were prepared by using a modified Brust's two-phase procedure [3]. The synthetic pathway was optimized and a 4.6:1 Au/S molar ratio was adopted for the preparation of hybrid **2**. Briefly, HAuCl_4 was transferred from water into dichloromethane by tetraoctylammonium bromide (TOAB), a quaternary alkyl-ammonium phase-transfer agent, which also acted as a de-protecting agent of the thioacetate Pd(II) complex **1**. After addition of BH_4^- , the hybrid system **2**, was obtained and characterized. Infrared spectra of hybrid **2**, confirmed the deprotection of the thiol with the disappearance of the carbonyl $\text{C}=\text{O}$ stretching mode.

UV–Vis spectra, collected for complex **1** and hybrid **2**, supported the hybrid formation. In particular, complex **1** showed an absorption band at 280 nm, while hybrid **2** exhibited a shielded plasmon resonance at about 510 nm. Preliminary photoluminescence measurements showed an emission band at 337 nm for both complex **1** and hybrid **2**. This result proves the possibility for gold nanoclusters to develop luminescence properties also in UV–Vis range.

The size, shape and crystalline structure of the functionalized gold nanoparticles are fundamental features for the future developments in technological applications. X-ray powder diffraction measurements (XRD) and high-resolution transmission electron microscopy (HR-TEM) allowed to characterize hybrid **2**.

The X-ray diffraction pattern of hybrid **2** shown in Fig. 1a, exhibits the characteristic Bragg peaks of the gold nanocrystals. The broadening of the Bragg peaks is due to the nanometer-size of the crystallites. In Fig. 1b, the simulation of the (111) and (200) peaks by a pseudo-Voigt function is reported. By using Scherrer's formula, from the full width of half-maxima (FWHM) of the most intense



Scheme 1. Chemical structure of Pd(II) organometallic complex, **1**, and synthesis of Pd(II) complex thiol–Au nanoparticle hybrid system, **2**.

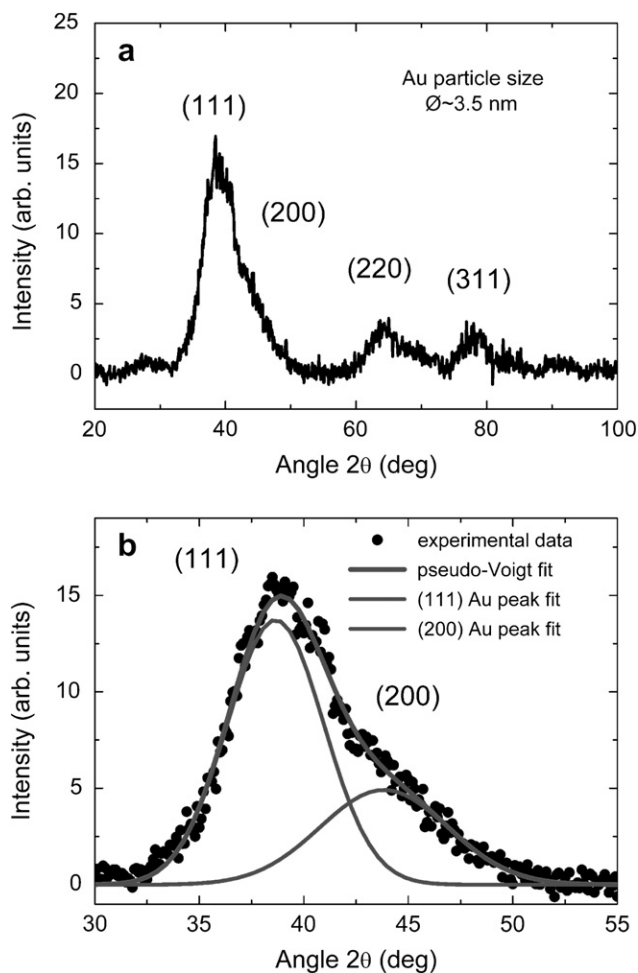


Fig. 1. (a) X-ray diffraction pattern of the hybrid **2** exhibiting distinct Bragg peaks due to the Au nanocrystallites and (b) simulation of the (111) and (200) peaks by a pseudo-Voigt function. Average Au particle size ($\varnothing \sim 3.5$ nm).

(111) Bragg peak the average particle diameter can be determined, which is 3.5 nm.

In Fig. 2a and b, TEM images of sample **2**, taken at different magnifications are reported. TEM observations show spherical shaped single-crystal gold particles and confirms the average diameter of the crystallites determined from XRD.

Fig. 2a gives an overview of the sample's features. Gold nanocrystals are distributed in zones, forming high and low density regions, and in some areas they may also aggregate in chains. From high-resolution TEM analysis (Fig. 2b), we can discriminate among elongated and spherical nanoparticles. Elongated nanoparticles are mainly due to a coalescence of two or more spherical nanoparticles which consist of single crystals. The inset of Fig. 2b shows a high-magnification image of one single gold nanocrystals. The spacing of the fringes is $d = 0.2$ nm and corresponds to the (200) Au lattice planes. Focusing on spherical nanoparticles, we obtained the size distribution reported in Fig. 2c, from which we can state that gold nanocrystals in this sample are uniform in size. The average size is of about 3–4 nm.

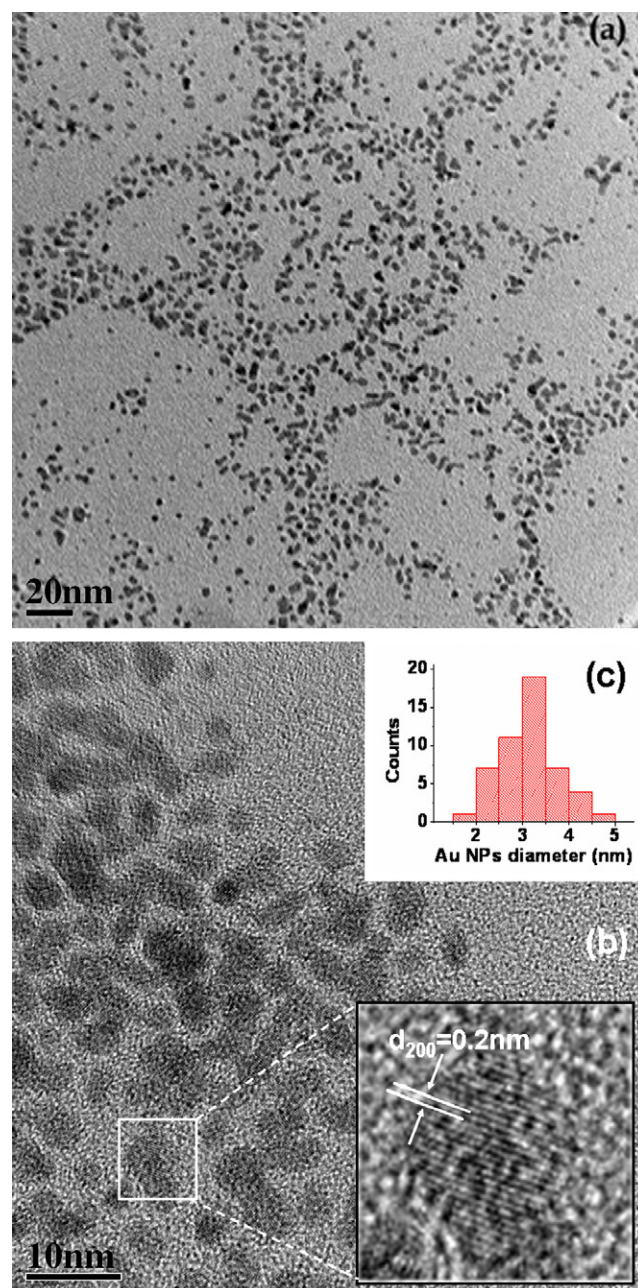


Fig. 2. Bright field TEM images of AuNPs of hybrid **2**, taken at different magnifications (a,b). The inset of (b) shows a high-resolution image of a single Au nanocrystal with well-defined (200) lattice fringes. Mean AuNPs size 3.2 nm (c).

The chemical environment of the functionalized Au nanoparticles and their interaction with the organothiols is at present under investigation by X-ray photoelectron spectroscopy (XPS) [14]. XPS measurements were carried out on sample **2** with the aim of finding a relationship between the Au(I)/S atomic ratio in the nanostructured assembly, which is indicative of the covalent Au–S link. To this purpose C1s, P2p, Pd4f, Au4f and S2p core level spectra have been collected and analyzed. The core level binding energy (BE) and full width at half-maximum (FWHM) were analyzed with particular attention to

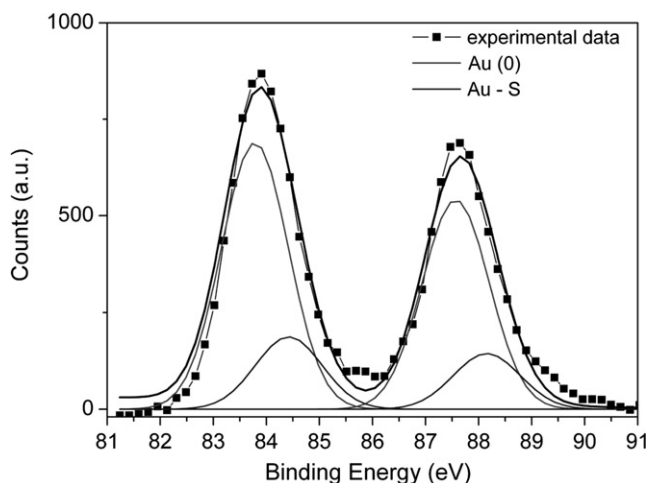


Fig. 3. XPS Au4f spectrum of hybrid **2**.

Au4f_{7/2} and S2p_{3/2} components, which are of main interest for the assessment of the Au–S bond. Evaluation of the atomic ratios of all the core spectra normalized to the S2p_{3/2} component led to assess that the molecular structure of complex **1** was clearly maintained in hybrid **2**.

By curve-fitting analysis, the Au4f spectrum, reported in Fig. 3, results from two pairs of spin–orbit components. The Au4f_{7/2} peak found at BE = 83.80 eV is attributed to metallic gold [15]; the second Au4f_{7/2} signal at higher BE values (BE = 84.42 eV) has been associated to Au atoms that are covalently bound to sulphur containing terminal groups. Semi-quantitative analysis of the XPS signals, allowed to estimate an atomic ratio 1:1 between the Au4f_{7/2} component at 84.42 eV and the S2p_{3/2} peak. This result is consistent with the formation of the hypothesized S–Au covalent bond, while some gold sites onto the surface of the nanoparticles seem not to be interacting with the thiols; this experimental result could be explained with the hindrance of the phosphine ligands linked to Pd(II) square planar complex.

3. Conclusions

In conclusion, we synthesized a new organometallic Pd(II) complex and the corresponding gold nanoparticle hybrid. XRD, TEM and XPS analyses confirmed the linking between Au and –S–Pd(PBu₃)₂(C≡CC₆H₅) moiety. The nanoparticles are homogeneous in size and structure and are uniformly functionalized by the organometallic complex.

The obtained hybrid could be a promising candidate for the achievement of new hybrid systems with extended electronic delocalization by varying the organic spacer bonded to Pd(II) centers. In fact, optical spectroscopy and electronic transport measurements are now under study in our laboratories in order to evaluate also potential device applications. These new materials open new perspectives in the field of thiols stabilized gold nanoparticles.

4. Experimental details

4.1. Material and methods

The reactions of complex **1** were performed under an inert argon atmosphere at room temperature (RT). Solvents were dried on Na₂SO₄ before use. Low conductivity water was obtained from Millipore Milli-Q water purification system. All chemicals, unless otherwise stated, were obtained from commercial sources and used as received. Palladium complex [PdCl₂(PBu₃)₂], i.e. *trans*-[dichlorobis(tributylphosphine)palladium(II)] was prepared by the following reported methods [16]. Phenylacetylene were purchased from Aldrich and distilled before use. Potassium thioacetate was purchased from Aldrich and used without further purifications. Preparative thin-layer chromatography (TLC) separation was performed on 0.7 mm silica plates (Merck Kieselgel 60 GF254) and chromatographic separations were obtained with 70–230 mesh silica (Merck), by using *n*-hexane/dichloromethane mixtures.

4.2. Synthesis of Pd(II) organometallic complex **1**

The organometallic complex [CH₃–CO–S–Pd(PBu₃)₂–C≡CC₆H₅] was prepared from square planar Pd(II) complex [Cl–Pd(PBu₃)₂C≡CC₆H₅] synthesized by the literature report [17], following a ligand substitution reaction, in the presence of potassium thioacetate in equimolar amount [11]. For a typical reaction, 1.5 mmol of [Cl–Pd(PBu₃)₂C≡CC₆H₅] were dissolved in CH₂Cl₂ (50 ml) and 1.8 mmol of CH₃–CO–SK were allowed to react at room temperature for 6 days.

The obtained solid was filtered and the spectroscopic characterizations follows: CH₃–CO–S–Pd(PBu₃)₂C≡CC₆H₅ (**1**): IR (film, cm⁻¹) ν(C≡C): 2113; ν(C=O): 1627; ν(C=C): 1602; UV (CH₂Cl₂, nm): 272.0 nm; ¹H NMR (CDCl₃ppm): 7.28 (d, 4H, Ar-*H*), 7.22 (d, 4H, Ar-*H*), 2.40 (s, CO–CH₃), 1.98 (m, 12H P–CH₂–), 1.59 (m, 12H, P–CH₂–CH₂–), 1.50 (q, 12H, P–CH₂–CH₂–CH₂–), 0.96 (t, 18H, –CH₃); ³¹P NMR (CDCl₃ppm): 10.40; Elemental analysis (%), found (calculated for C₃₄H₆₂P₂PdSO): C = 59.03 (59.42); H = 9.12 (9.09); S = 5.07 (4.67).

4.3. Synthesis of Pd(II) organometallic complex-stabilized gold nanoparticles **2**

The stabilized gold nanoparticles were prepared by two-phase procedure [10] using a 4.6:1 Au/thiol reactant molar ratio. A 0.03 M aqueous solution of HAuCl₄ · H₂O (1.12 mmol) was added to a solution of [CH₃–CO–S–Pd(PBu₃)₂C≡CC₆H₅] (0.243 mmol) in 80 ml of dichloromethane (DCM). A quaternary alkyl-ammonium phase-transfer, 1.6 g of tetraoctylammonium bromide (TOAB), was added to transfer HAuCl₄ from water into organic phase. The gold was reduced with a 0.4 M aqueous solution of NaBH₄ (30.8 ml) added over a period of

1 min. The system reacted at room temperature for 3 h. Then 50 ml of H₂O and 50 ml of CH₂Cl₂ were added and the organic phase was separated and dried over anhydrous Na₂SO₄. The drying agent and any insoluble materials were removed by filtration and the solution was reduced to a solid, *in vacuo*. The dark brown residue was resuspended in methanol. The suspension was filtered over celite and subsequently washed with 400 ml of acetonitrile and 400 ml of hexane to remove any excess of arenethiolate, TOAB and by-products. The solid was washed off from the celite with DCM, the solvent was removed *in vacuo* and the product was dried *in vacuo* overnight. The product was highly soluble in CH₂Cl₂ and CHCl₃.

4.4. Instrumentation

FTIR spectra were recorded as nujol mulls or as films deposited from CHCl₃ solutions by using CsI cells, on a Bruker Vertex70 Fourier Transform spectrometer.

¹H, ³¹P NMR spectra were recorded on a Bruker AC 300P spectrometer at 300 and 121 MHz respectively, in appropriate solvents (CDCl₃); the chemical shifts (ppm) were referenced to TMS for ¹H NMR assigning the residual ¹H impurity signal in the solvent at 7.24 ppm (CDCl₃). ³¹P NMR chemical shifts are relative to H₃PO₄ (85%). UV–Vis spectra were recorded on a Varian Cary 100 instrument. UV measurements were performed at room temperature using quantitative solutions of the compounds in CH₂Cl₂. UV–Vis spectra were recorded on a Cary 100 Varian instrument. Photoluminescence spectra were performed on a Perkin–Elmer LS 50 Fluorescence Spectrometer. All measurements were performed at room temperature using quantitative solutions in CHCl₃ (1 mg/ml).

XPS spectra were obtained using a custom designed spectrometer. A non-monochromatised Mg K α X-rays source (1253.6 eV) was used and the pressure in the instrument was maintained at 1×10^{-9} Torr throughout the analysis. The experimental apparatus consists of an analysis chamber and a preparation chamber separated by a gate valve. An electrostatic hemispherical analyzer (radius 150 mm) operating in the fixed analyzer transmission (FAT) mode and a 16-channel detector were used. The film samples were prepared by dissolving our materials in CHCl₃ and spinning the solutions onto polished stainless steel substrates. The samples showed good stability during the XPS analysis, preserving the same spectral features and chemical composition. The experimental energy resolution was 1 eV on the Au 4f_{7/2} component. The resolving power $\Delta E/E$ was 0.01. Binding energies (BE) were corrected by adjusting the position of the C1s peak to 285.0 eV in those samples containing mainly aliphatic carbons and to 284.7 eV in those containing more aromatic carbon atoms, in agreement with literature data [18]. The C1s, Pd3d, Pt4f, P2p, Cl2p spectra were deconvoluted into their individual peaks using the *Peak Fit*

curve-fitting program for PC. Quantitative evaluation of the atomic ratios was obtained by analysis of the XPS signal intensity, employing Scofield's atomic cross-section values [19] and experimentally determined sensitivity factors.

The XRD measurements were performed by using a high-resolution X-ray diffractometer (HRD3000 Ital Structures) in parallel beam optical configuration (Max-FluxTM Optical System). A Copper-target ($\lambda_{\text{Cu K}\alpha} = 0.154056$ nm), with a X-ray generator setting of 30 mA/40 kV, was employed as X-ray source (fine focus X-ray tube).

For the structural characterization of the nanoparticles few drops of the diluted solutions were deposited on polished (100)-Si surfaces and dried in air. The X-ray diffraction patterns were recorded in glancing incidence conditions, i.e. the angle between the incident X-ray beam and the “nanoparticle film” surface was kept constant at $\omega = 1.0^\circ$, while the X-ray intensity was measured by 2θ -scans of the detector-system. The average crystallite size was estimated from the diffraction peak broadening, pseudo-Voigt function fitting and applying the Scherrer's formula.

The samples were studied by HRTEM and diffraction contrast imaging. All images were recorded with a FEI TECNAI G2 F30 Supertwin field-emission gun scanning transmission electron microscope (FEG STEM) operating at 300 kV and with a point-to-point resolution of 0.205 nm. TEM specimens were prepared by depositing few drops of the diluted solutions on carbon coated TEM grids to be directly observed.

Acknowledgements

The authors gratefully acknowledge the financial support of MIUR (Rome, Italy) and of Regione Puglia (Bari, Italy) to this research work.

References

- [1] J.C. Love, L.A. Estroff, J.K. Kriebel, R.G. Nuzzo, G.M. Whitesides, *Chem. Rev.* 105 (2005) 1103.
- [2] M.C. Daniel, D. Astruc, *Chem. Rev.* 104 (2004) 293.
- [3] M. Brust, M. Walker, D. Betell, D.J. Schiffrin, R. Whyman, *J. Chem. Soc., Chem. Commun.* (1994) 801.
- [4] A.C. Templeton, W.P. Wuelfing, R.W. Murray, *Acc. Chem. Res.* 33 (2000) 27.
- [5] C.N.R. Rao, G.U. Kulkarni, P.J. Thomas, P.P. Edwards, *Chem. Eur. J.* 8 (2002) 28.
- [6] S.R. Johnson, S.D. Evans, S.W. Mahon, A. Ulman, *Langmuir* 13 (1997) 51.
- [7] R. Shenhar, V.M. Rotello, *Acc. Chem. Res.* 36 (2003) 549.
- [8] S. Chen, R.W. Murray, *Langmuir* 15 (1999) 682.
- [9] R.C. Price, R.L. Whetten, *J. Am. Chem. Soc.* 127 (2005) 13750.
- [10] M. Busby, C. Chiorboli, F. Scandola, *J. Phys. Chem. B* 110 (2006) 6020.
- [11] Y.C. Neo, J.J. Vittal, T.S.A. Hor, *J. Organomet. Chem.* 637–639 (2001) 757.
- [12] I. Fratoddi, C. Battocchio, A. La Groia, M.V. Russo, *J. Polym. Sci., Polym. Chem.* 45 (2007) 3311.
- [13] W.-Y. Wong, *Coord. Chem. Rev.* 249 (2005) 971.

- [14] M. Buttner, H. Kroger, I. Gerhards, D. Mathys, P. Oelhafen, *Thin Solid Films* 495 (2006) 180.
- [15] NIST X-ray Photoelectron Spectroscopy Database, NIST Standard Reference Database 20, Version 3.4.
- [16] G.B. Kauffman, L.A. Teter, *Inorg. Synth.* 7 (1963) 245.
- [17] K. Sonogashira, S. Kataoka, S. Takahashi, N. Hagihara, *J. Organomet. Chem.* 160 (1978) 319.
- [18] G. Beamson, D. Briggs, *High Resolution XPS of Organic Polymers, the Scienta ESCA300 Database*, Wiley, New York, 1992.
- [19] J.M. Scofield, *J. Electron Spectrosc. Relat. Phenom.* 8 (1976) 129.